

EXTENDING HARP IMAGING BY ACQUIRING AN OVERDETERMINED SET OF STRIPES

Lucilio Cordero-Grande¹, and Carlos Alberola-López¹

¹University of Valladolid, Valladolid, Castilla y León, Spain

Introduction

MR tagging allows the tracking of material points through time. This is of special relevance, for instance, in the analysis of myocardial local motion, whose anomalies are directly related with impaired cardiac function. The HARP method for MR tagging allows the dense reconstruction of the deformation gradient tensor [1]. Nevertheless, without a proper reconstruction scheme, it is prone to be corrupted by noise and phase interferences due to the application of a gradient operator on the reconstructed phase. Here, we propose an extension of this method based in the acquisition of an overdetermined set of stripe patterns, as usually applied in DTI [2], which, especially when combined with our previous contribution in [3], is able to avoid the orientation and spacing dependent phase interferences.

Method

The commonly used SPAMM technique for MR tagging is based on the application of a spatial modulation with wave vector $\mathbf{k}_i = k_i \mathbf{u}_i$, with k_i its wave number and \mathbf{u}_i its orientation. For simplicity, we focus on the reconstruction of 2D HARP images and in 1-1 SPAMM. Nevertheless, extensions to other scenarios are straightforward. In this paper we extend the reconstruction equations for the deformation gradient tensor in [1] (where 2 wave vectors are used) in those cases in which a set of $I \geq 2$ wave vectors are applied. Let $\mathbf{k}_i^T = k_i(u_0, u_1)$, with $1 \leq i \leq I$ be this set of vectors. They can be arranged in matrix form as $\mathbf{K}^T = (\mathbf{k}_1 \ \mathbf{k}_2 \ \dots \ \mathbf{k}_I)$. Now suppose that $\phi(\mathbf{x})$ is the HARP image for the wave vector \mathbf{k}_i . The (spatial) deformation gradient tensor $\mathbf{f}(\mathbf{x}) = [\partial \mathbf{x} / \partial \mathbf{x}](\mathbf{x})$ is related with the gradient of the image $\phi_i(\mathbf{x})$ by $\mathbf{k}_i^T \mathbf{f}(\mathbf{x}) = [\partial^* \phi_i / \partial \mathbf{x}](\mathbf{x}) = \min\{\partial \phi_i / \partial \mathbf{x}](\mathbf{x}), \partial W(\phi_i + \pi) / \partial \mathbf{x}](\mathbf{x})\}$, with $W(\cdot)$ the wrapping operator, which maps its argument in the interval $[-\pi, \pi]$ [1]. Rearranging the gradient of the images in matrix form, $\mathbf{Y}^T(\mathbf{x}) = ([\partial^* \phi_1 / \partial \mathbf{x}]^T(\mathbf{x}) \ [\partial^* \phi_2 / \partial \mathbf{x}]^T(\mathbf{x}) \ \dots \ [\partial^* \phi_I / \partial \mathbf{x}]^T(\mathbf{x}))$, one has $\mathbf{Y}(\mathbf{x}) = \mathbf{K} \mathbf{f}(\mathbf{x})$. In order to estimate $\mathbf{f}(\mathbf{x})$, a possibility is to resort to the Least Squares (LS) method, so $\mathbf{f}(\mathbf{x}) = (\mathbf{K}^T \mathbf{K})^{-1} \mathbf{K}^T \mathbf{Y}(\mathbf{x})$. However, taking into consideration that phase interferences correspond to outliers in the $\mathbf{f}(\mathbf{x})$ estimation, our proposal is to resort to the Least Absolute Deviation (LAD) method, due to its robustness. Hence, the reconstruction is performed iteratively by $\mathbf{f}^{i+1}(\mathbf{x}) = (\mathbf{K}^T \mathbf{W}(\mathbf{x}) \mathbf{K})^{-1} \mathbf{W}(\mathbf{x}) \mathbf{K}^T \mathbf{Y}(\mathbf{x})$, with $\mathbf{W}^i(\mathbf{x})$ a diagonal weight matrix obtained by $\mathbf{W}^i_{i,i}(\mathbf{x}) = [\sum_m (Y_{i,m}(\mathbf{x}) - \sum_n K_{i,n} f_{n,m}^i(\mathbf{x}))^2]^{1/2}$ and establishing $\mathbf{f}^i(\mathbf{x}) = \mathbf{Id}$, with \mathbf{Id} the identity matrix. Finally, as for the computation of the local phase image $\phi_i(\mathbf{x})$, we propose to use the methodology introduced in [3], based on the Windowed Fourier Transform (WFT).

Results

The simulated deformation proposed in [4] has been used for validation, but applied to a real image in order to better reproduce the spectral content of real data. The image corresponds to a medial slice for the end-diastolic phase of a cine echo-like SSFP MR cardiac acquisition. A GE Genesis Sigma 1.5T equipment has been used. Image dimensions are 512×512 and its resolution is $0.86 \times 0.86 \text{ mm}^2$, with a thickness of 6mm. Some modifications have been performed on the deformation in [4] to consistently apply it to the real image. Specifically, in our case $z=20 \text{ mm}$ and $R_o=60 \text{ mm}$, we have nulled the dependence of the angular parameter with R for $R_i \leq R$ and $R \leq R_o$ and the corresponding term now reads $\phi(-(R-R_i)(R-R_o))^{1/2}$ for $R_i \leq R \leq R_o$. Moreover, the fluctuating blood motion effect is represented by decreasing the magnetization contrast to a 10% of its original value outside the myocardium. We have performed a set of experiments in which we estimate $\mathbf{f}(\mathbf{x})$ and measure the mean Fréchet Norm Error (FNE) between reconstructed and synthetic tensors for the pixels inside the myocardium. The filter bandwidth for HARP extraction is selected to be $\text{BW}=0.35k_i$ and the analysis window has a Gaussian form with a size of 32×32 pixels (see [3]). The reconstruction is applied to a set of wave vectors which span the plane uniformly and have a common spacing. Results are included in Fig. 1 for different spacings. LS and LAD reconstructions are compared. The iterative process in LAD reconstruction is finished when two consecutive estimations of $\mathbf{f}(\mathbf{x})$ differ less than 10^{-3} among all pixels and components. The main conclusions are (1) LAD reconstruction outperforms LS one for $I \geq 4$, (2) Overdetermined HARP (O-HARP) using LAD reconstruction improves the performance with respect to conventional HARP for $I \geq 4$ and (3) for a stripe spacing of 6mm, a relative decrease in the mean FNE of a 55% has been observed for $I=6$ (mean FNE of 0.1352) with respect to $I=2$ (mean FNE of 0.2981), which shows the great potential of the O-HARP strategy. Finally, in Fig. 2 we compare different methodologies for the reconstruction of $\mathbf{f}(\mathbf{x})$. On one hand, we compare an O-HARP acquisition with 7 orientations both for 5.5mm and 6mm spacing (so $I=14$) and a conventional one with $I=2$ and spacing of 6mm. On the other hand, we compare the original FT-based method for HARP reconstruction [1] against the WFT-based one [3]. The major visual conclusion is that the O-HARP acquisition avoids the presence of outliers whereas the WFT-based filtering improves the mean level of agreement between the estimated and the original $\mathbf{f}(\mathbf{x})$.

Discussion and conclusions

A method for the reconstruction of the deformation gradient tensor is presented which builds upon the acquisition of an overdetermined set of stripes in order to limit the influence of the outliers derived from the combination of phase interferences and the gradient operation. The method has considerably improved the precision in the estimated tensor for an analytic model of myocardial deformation. We believe that this methodology brings new opportunities in the design of SPAMM acquisition sequences for HARP imaging, especially when combined with modern acquisition protocols such as [5]. The overload introduced by gathering an overdetermined set of stripes can be compensated by the acquisition of a reduced subset of the k -space in order to reconstruct the local phase [6]. Finally, we believe that these ideas can also be applied with slight modifications to DENSE or even PC acquisitions [7]. With these considerations in mind, new families of acquisition protocols can potentially be designed for motion sensitive MR imaging, which could simultaneously improve the resolution, robustness and precision in the analysis of motion.

References

1. Osman, N.F., McVeigh, E.R., Prince, J.L., *IEEE Trans. Med. Imag.*, 19(3):186-202; 2000.
2. Le Bihan, D., Mangin, et al., *J. Magn. Res. Imag.*, 13:534-546; 2001.
3. Cordero-Grande, L., Vegas-Sánchez-Ferrero, et al., *IEEE ISBI*: 520-523; 2011.
4. Marinelli, M., Positano, V., et al., *IEEE ISBI*: 1429-1432; 2008.
5. Rutz, A.K., Ryf, S., et al., *Magn. Res. Med.*, 59:755-763; 2008.
6. Sampath, S., Derbyshire, et al., *ISMRM*: 111; 2001.
7. Kuijper, J.P.A., Hofman, et al., *J. Magn. Res. Imag.*, 24:1432-1438; 2006.

Acknowledgements: This work was partially supported by the MICINN and the FEDER under Research Grant TEC2010-17982, and by the CDTI under the cvREMOD project and Research Grant CEN-20091044. The work was also funded by the Junta de Castilla y León under Grants VA039A10-2 and VA376A11-2 and the Consejería de Sanidad de Castilla y León under Grants GRS 292/A/08, SAN126/VA032/09 and SAN126/VA033/09.

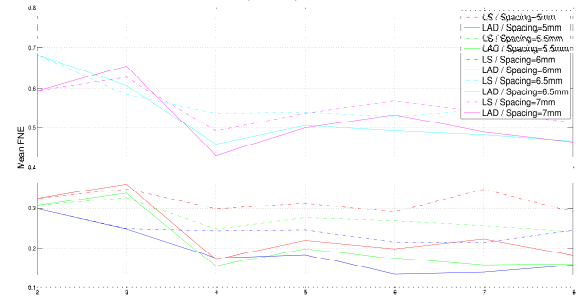


Fig. 1. Mean FNE

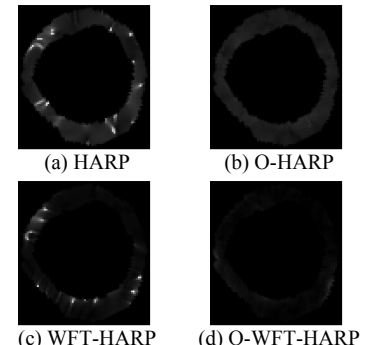


Fig. 2. Distribution of the FNE